Polymer 50 (2009) 3204–3210

Contents lists available at ScienceDirect

Polymer

journal homepage: www.elsevier.com/locate/polymer

Colloidal gel from amphiphilic heteroarm polyelectrolyte stars in aqueous media

Apostolos Kyriazis [a,b], Thierry Aubry [c], Walther Burchard [d], Constantinos Tsitsilianis [a,b,*]

[a] Department of Chemical Engineering, University of Patras, 26504 Patras, Greece
[b] Institute of Chemical Engineering and High Temperature Chemical Processes, ICE/HT-FORTH, P.O. Box 1414, 26504 Patras, Greece
[c] Université Européenne de Bretagne, LIMATB Equipe Rhéologie, 6 avenue Victor Le Gorgeu, CS 93837, 29238 Brest Cedex 3, France
[d] Institut für Makromolekulare Chemie, Albert Ludwigs Universität, 79104 Freiburg i. Br., Germany

ARTICLE INFO

Article history:
Received 18 December 2008
Received in revised form
21 April 2009
Accepted 23 April 2009
Available online 14 May 2009

Keywords:
Amphiphilic star polyelectrolyte
Coloidal gel
Jamming effect

ABSTRACT

We report on the gelation capability of polystyrene/poly(2-vinyl pyridine) amphiphilic heteroarm polyelectrolyte stars in acidic salt-free aqueous media. The star polymers associate through hydrophobic interactions, by retraction of the stretched arms under no interdigitation conditions, in the dilute regime forming colloidal soft nanoparticles comprising about 6 stars, At concentrations significantly higher than the hydrodynamic overlap concentration ($c > 40c^*$), the crowding of the colloidal nanoparticles drives a jamming transition, leading to a colloidal gel. The intermediate overlap regime ($c^* < c < 40c^*$) is characterized by a significant compaction of the polyelectrolyte entities prior interdigitation and jamming.

1. Introduction

Amphiphilic diblock copolymers undergo self-organization in aqueous media forming micellar nanostructures of various morphologies. In an asymmetric diblock with short hydrophobic block, the adopting self-assembly structure is that of a star-shaped polymer in which all the branched chains are chemically linked in a central nodule. Thus the star-like micelles can be considered as physically linked star polymers. At elevated concentrations both types exhibit interesting rheo-thickening effects and can be used as rheology modifiers in various applications [1,2]. Recently, an increasing attention focus to the star polymers because they are model branched systems with both polymeric and colloidal properties which can be tuned through their functionality [3].

Most star polymers studied in the literature are uncharged flexible macromolecules, whose static and dynamic properties have been investigated both theoretically [4,5] and experimentally [6,7]. As far as static solution properties are concerned, it has been established that the stretching of the arms, due to inter-arm repulsive interactions, delays interpenetration of stars above the overlap concentration [8]. As far as dynamic properties are concerned, the viscoelastic properties of star polymer systems have been shown to depend on the number of arms. At low arm number (up to ~15), the viscoelastic properties of star polymers depend on the arm molecular weight but not on the arm number, and the arm relaxation governs the dynamics [9]. At higher arm number (from ~30), the motion of the center of mass of the whole star was shown to contribute also to the stress relaxation [10].

Star-shaped polyelectrolytes, i.e. star polymers with charged arms, exhibit specific behavior in high dielectric permittivity media due to the additional electrostatic interactions arisen from the dissociation of the ionizable groups along the arms. In salt-free aqueous solutions, the arms of a polyelectrolyte star of high degree of ionization, adopt a stretched conformation. This physical picture is mainly governed by entropic effects due to the trapped counterions within the star interior. The degree of arm stretching is determined by the balance between the osmotic pressure of the free counterions inside the star and the entropic elasticity of the arms (osmotic regime) [11,12].

Moreover, stars made of polyelectrolyte chains have been shown to interdigitate at concentrations well above the overlap concentration [13]. A complete diagram of concentration regimes of salt-free aqueous polyelectrolyte star solutions has been proposed quite recently by Shusharina and Rubinstein, using scaling concepts [14].

Heteroarm star copolymers are a special class of star-shaped polymers bearing equal number of two different in nature pure arms [15]. In previous studies preliminary results have shown that amphiphilic stars constituted of hydrophobic and polyelectrolyte arms form very viscous aqueous systems at low concentrations [16,17]. In this work, we explore the ability of an

* Corresponding author. Tel.: +30 2610969531; fax: +30 2610997266.
E-mail address: ct@chemeng.upatras.gr (C. Tsitsilianis).

0032-3861/$ – see front matter © 2009 Elsevier Ltd. All rights reserved.
doi:10.1016/j.polymer.2009.04.076

amphiphilic heteroarm star copolymer, constituted of pure polystyrene and poly(2-vinyl pyridine) arms, PS_8P2VP_8 (Scheme 1), to form a colloidal gel in acidic salt-free aqueous media in which the P2VP arms behave like weak polyelectrolytes due to protonation of the pyridine repeating units. The ability to tune the rheological properties of the model system studied in this work with molecular or external conditions, such as number and size of the arms, pH or ionic strength, is of particular interest for potential applications.

2. Experimental part

2.1. Synthesis

The PS_8–$P2VP_8$ heteroarm star copolymer was prepared via a three-step sequential "living" anionic polymerization procedure ("In–Out" method) using divinylbenzene linkage (DVB) [18]. In the first step the polystyrene arms were prepared using *sec*-butyl lithium as the initiator at −40 °C in THF. After the consumption of the styrene monomer and sampling out, a small amount of divinylbenzene was added to the reaction medium. Star-shaped polystyrene (PS_n) was thus formed, part of which was deactivated and sampled out for the purpose of characterization. The rest "living" star polymer was used to initiate the polymerization of a chosen amount of 2-vinyl pyridine that was added to the reaction medium at −75 °C. After complete polymerization of 2-vinyl pyridine the reaction mixture was deactivated with degassed methanol and the final product was recovered by precipitation in cold heptane, dried, redissolved in benzene and freeze-dried.

2.2. Sample preparation

The samples were prepared in filtered (0.45 μm) 0.01 N HCl under stirring for 18 h. Subsequently they were heated at 100 °C for 72 h and allowed to equilibrate at room temperature for 24 h. Prior to the measurements the pH was checked, and corrected if necessary at pH 2 by adding HCl. Finally the solutions used for the light scattering experiments were filtrated with 0.45 μm filters in order to become dust free.

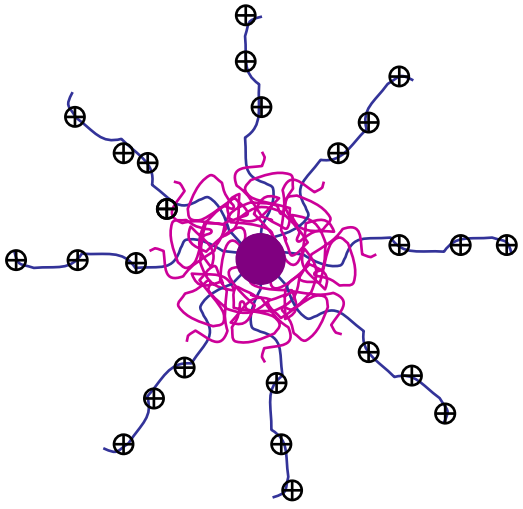

Scheme 1. Schematic representation of the PS_8P2VP_8 amphiphilic heteroarm polyelectrolyte star in acidic aqueous environment. The PS arms collapse on the core whereas the charged P2VP arms adopt a stretched conformation. Part of the P2VP arms located in the vicinity of the star core remains uncharged.

2.3. Rheological experiments

Steady and oscillatory simple shear measurements have been performed with a Rheometric Scientific SR-200 controlled stress rheometer, using either a cone-plate geometry (diameter 25 mm, cone angle 0.1 rad) for samples with high viscosity, or a Couette geometry (outer cylinder diameter 31.7 mm, inner cylinder diameter 29.5 mm) for low viscosity samples. All steady shear apparent viscosity results were obtained on time scales long enough for the transient viscosity variations to be negligible. A thin layer of low viscosity silicone oil was put on the air/sample interface in order to minimize solvent evaporation. All experiments have been carried out at 25 ± 0.01 °C, using a water bath circulator.

2.4. Light scattering experiments

2.4.1. Static light scattering

The weight average molecular weight of the PS_n star precursor and PS_nP2VP_n was determined by static light scattering using a thermally regulated (±0.1 °C) spectrogoniometer model BI-200SM (Bruckhaven) equipped with a He–Ne laser (632.8 nm). The refractive index increment dn/dc, required for the interpretation of the light scattering measurements, was calculated by using the known values of each block and the monomer composition. Data were treated by the standard Zimm method using the equation

$$\frac{Kc}{R_\theta(q,c)} = \frac{1}{p(q,c)}\left(\frac{1}{M_w} + 2A_2c + \cdots\right) \quad (1)$$

where $K = 4\pi^2 n^2 (\mathrm{d}n/\mathrm{d}c)^2/\lambda^4 N_A$ is a constant containing the refractive index n of the solvent, refractive index increment of the polymer with respect to the solvent, dn/dc, wavelength of the incident light, λ, and the Avogadro constant, N_A. The other symbols stand for: $R_\theta(q,c)$ is the corrected Rayleigh ratio, which depends on the polymer concentration and on the scattering vector $q = (4\pi n/\lambda)\sin(\theta/2)$, M_w is the weight average molar mass of scattering polymeric particles and A_2 is the "light-scattering-weighted" second virial coefficient of the concentration expansion. The molecular characteristics of the polymer under investigation are summarized in Table 1.

2.4.2. Dynamic light scattering

Auto-correlation functions $g(q,t)$ were measured at a given wave vector, q, on a broad time scale with a full multiple digital correlator (ALV-5000/FAST) equipped with 280 channels. The light source was an Argon-Ion laser (Spectra Physics 2020) operating in single mode at 671 nm with a constant output power of about 220 mW. The correlation functions were analyzed by the constrained regularized CONTIN method through CoVA-Jacek Gapinski 2001 software. The hydrodynamic radii were determined via the Stokes–Einstein equation

$$R_h = k_B T/(6\pi\eta D) \quad (2)$$

Where $D = \Gamma/q^2$ is the diffusion coefficient of the scattered dispersed particles, k_B is the Boltzmann constant and η is the viscosity of the solvent at temperature T.

3. Results and discussion

In the present paper rheological and light scattering experiments were conducted in aqueous media at pH 2 and 25 °C. Under these conditions the PS arms collapse and form glassy hydrophobic nanodomains whereas the P2VP arms are charged through protonation (degree of protonation 60%) [17] and adopt a stretched

Table 1
The molecular characteristics of the heteroarm star copolymer.

Sample	$\overline{M}_{w,arm} \times 10^{-3}$	$\overline{M}_w/\overline{M}_n$[a] arm	$\overline{M}_w/\overline{M}_n$[a] star	$\overline{M}_p \times 10^{-3}$[a]	$\overline{M}_w \times 10^{-3}$(LS)	f[b]
PS_8 precursor	19.0[a]	1.09		100	173	8.5
PS_8P2VP_8	22.7[c]		1.11	140	366	17.0

[a] By GPC.
[b] Mean number of arms determined by SLS.
[c] M_n of P2VP arms calculated by the formula $[M_w(PS_8P2VP_8) - M_w(PS_8)]/f$.

conformation. Due to the glassy PS arms, the samples were heated at 100 °C (non-frozen conditions) for prolonged time prior to use in order to aid reorganization and homogenization of the system.

3.1. Low concentration regime

In order to explore possible star association effects and to characterize the size of the self-assembled entities present at low concentrations, static and dynamic light scattering experiments were performed first.

In Fig. 1 the inverse scattering intensity data, expressed as $Kc/R_\theta(q,c)$ and extrapolated to the zero scattering vector, are plotted as a function for concentrations $c \leq 0.01$ wt%. From the fluctuation theory we know that the scattering intensity at zero scattering angle is given by the osmotic compressibility:

$$RTc(\partial c/\partial \pi) = R_{\theta=0}(c)/\mathrm{K} \tag{3}$$

which can be expanded in a virial series:

$$\frac{Kc}{R_{\theta=0}} = \frac{1}{M_w}\left(1 + 2A_2M_wc + 3A_3M_wc^2 + \cdots\right) \equiv \frac{1}{M_{app}(c)} \tag{4}$$

For an associating system the molar mass will increase with the concentration. Thus we have

$$\frac{M_w(c)}{RT}\left(\frac{\partial \pi}{\partial c}\right) = \frac{M_w(c)}{M_{app}(c)} = \left(1 + 2X + 3a_2X^2 + \cdots\right) \tag{5}$$

where

$$X = A_2M_wc = c/c^*_{A2} \tag{6a}$$

and c^*_{A2} the thermodynamic overlap concentration

$$c^*_{A2} = 1/(A_2M_wc) \tag{6b}$$

From the static light scattering data the molecular weight was found to be $M_w = 2.273 \times 10^6$ g/mol, which reveals the formation of micellar self-assemblies of very low average association number ($N = 6.2$), in good agreement with previous results reported for similar heteroarm stars [17,19,20]. Moreover, the thermodynamic overlap concentration deduced from Eq. (6b) was determined at 0.03 mg/mL.

The concentration dependence of the linear and quadratic coefficients, from the curves of Fig. 1a, as shown in Fig. 2, is remarkable. The convex curvature in the q^2-dependence of the scattering curves apparently becomes stronger with increasing concentration, but is a continuous function. The two highest concentrations were not included, since a striking change occurred with no detectable curvature. Anyway, the initial slope increases by 35% when c increases up to 0.02 mg/mL, whereas it drastically decreases above $c > 0.02$ mg/mL. This behavior can be attributed to a remarkable change in the structure of the scattering entities, since the initial slope determines the apparent radius of gyration, given by:

$$R^2_{g,app}(c) \equiv 3 \cdot M_{app}(c) \cdot \text{inital slope}(c) \tag{7}$$

Together with Eqs. (4) and (5) this relationship can be combined with the actual mean square radius of gyration to give:

$$R^2_g(c) = R^2_{g,app}(c)\,\frac{M_w(c)}{M_{app}(c)} \tag{8}$$

a relationship which directly follows from Zimm's famous equations [21].

Fig. 3 shows the concentration dependence of the apparent radius of gyration and the true one that was corrected in order to take into account the repulsive interactions. $R_{app}(c)$ decreases when c increases as observed for most polymers. As far as the actual radius of gyration is concerned, the results show an increase of the dimensions of the macromolecular entities, at least up to 0.01 mg/mL.

However, for the samples at 0.05 and 0.1 mg/mL, which are clearly above c^*_{A2}, a pronounced decrease of the actual radius of gyration is observed. The behavior at $c < c^*_{A2}$ may be caused by chain stiffening due to electrostatic interactions between non-touching

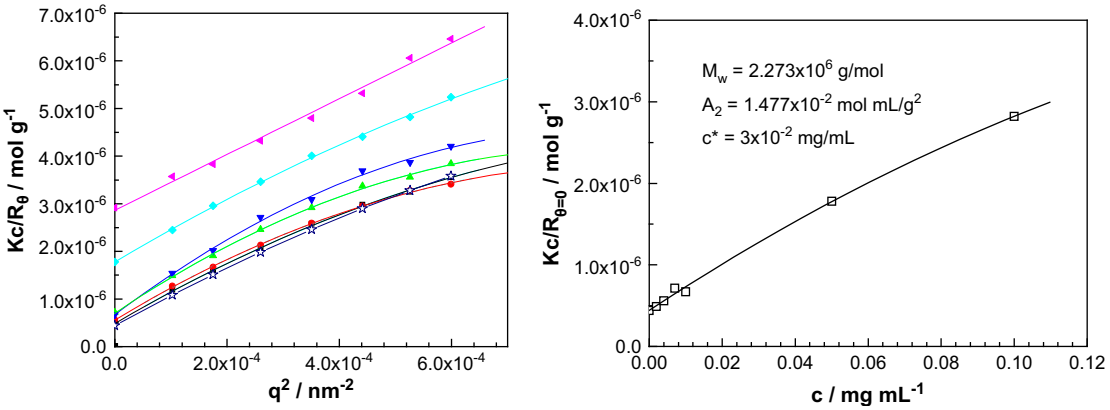

Fig. 1. (a) Angular dependence of the $Kc/R_\theta(q,c)$ at 6 different concentrations and (b) concentration dependence of the $Kc/R_{\theta=0}(c) = 1/M_{app}$ (c) extrapolated to zero angle of the PS_8P2VP_8 aqueous solution at pH 2 and at 25 °C.

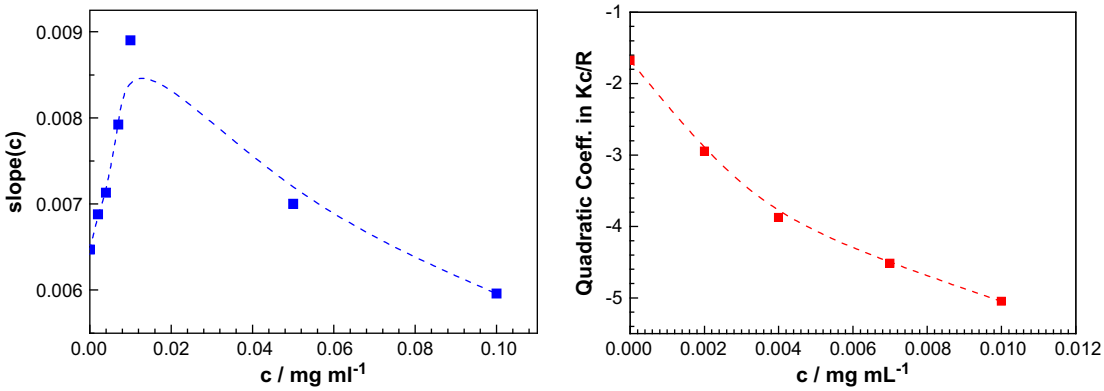

Fig. 2. Concentration dependence of the linear (a) and quadratic coefficients (b), from the curves of Fig. 1a.

neighbors, but once c^*_{A2} is exceeded a compression or shrinking of the structure is induced. This shrinkage has mainly a thermodynamic origin, due to the osmotic pressure on particles which prevent them from inter-penetration, but may also have an electrostatic origin, due to a screening effect of interactions.

A characteristic autocorrelation function, along with the distribution of relaxation times (through CONTIN analysis), is depicted in the inset of Fig. 4. A monomodal distribution of relaxation times was obtained in all cases which should be attributed to the diffusion of aggregates of mean hydrodynamic radius $R_H = 126$ nm, as calculated by the Stokes–Einstein formula (Eq. (2)) for equivalent hard spheres.

More importantly, as R_H exceeds the fully stretched length of the PS and P2VP arms (*ca.* 100 nm) and as the ratio $R_g/R_H = 1.66$ ($R_g = 210$ nm from the extrapolated value at zero angle, Fig. 3) is considerably higher than unity, then the formed nanoparticles are expected to adopt a non-spherical shape, but rather an ellipsoidal one [16,22].

Therefore a plausible morphology of the charged self-assembly, which is formed below the overlap concentration, is an ellipsoid soft nanoparticle constituted of about six amphiphilic stars associated through the attractive interactions of the hydrophobic PS arms located in the vicinity of the star core. Due to the glassy character of the arms, these self-assemblies must be considered as frozen. These interactions are possible because the star cores of neighboring interacting stars can approach each other by retraction of the stretched arms under no interdigitation conditions, as molecular dynamic simulations have shown [23]. Direct experimental observations through Cryo-TEM have provided evidence that spherical polyelectrolyte brushes, which resemble the amphiphilic star under investigation (Scheme 1), do not interdigitate in the osmotic regime [24].

It seems therefore that the physical picture of the system under investigation is rather a suspension of charged colloidal soft nanoparticles, which are entities between star and brush polyelectrolytes, bearing a hydrophilic layer of about 50 stretched chains in the osmotic regime (Scheme 2) [25].

Knowing the mean hydrodynamic radius of the nanoparticles, the hydrodynamic overlap concentration, c^*_{Rh} can be inferred (Eq. (9)). At c^*_{Rh}, the stars fill the available space without interpenetration:

$$c^*_{Rh} = \frac{3M_w}{4\pi N_a R_H^3} \cong 0.046 \text{ wt\%} \quad (9)$$

The fact that the thermodynamic and hydrodynamic overlap concentrations differ remarkably, should be attributed to the polyelectrolyte nature and the anisotropic structure of the soft nanoparticles.

3.2. High concentration regime

Dynamic light scattering experiments were performed above c^*_{Rh} in order to explore the dynamics of the system when crowding

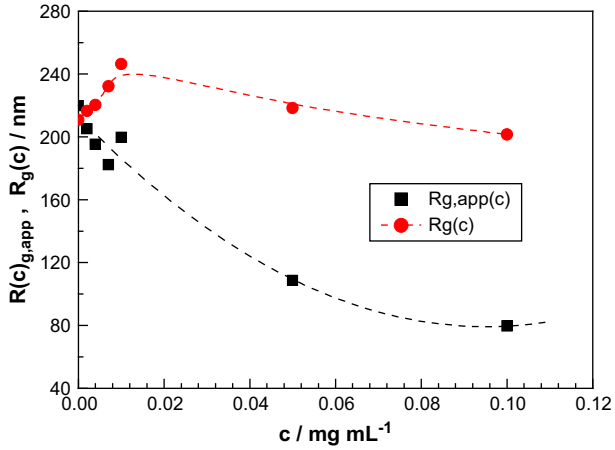

Fig. 3. Concentration dependence of the apparent radius of gyration $R_{app}(c)$ and the actual radius of gyration $R_g(c)$.

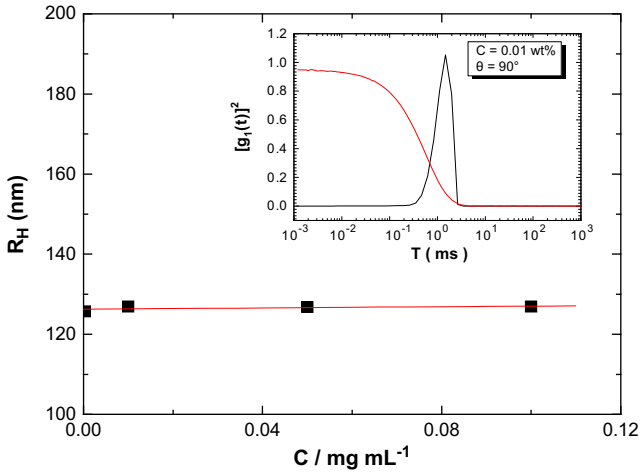

Fig. 4. Concentration dependence of the hydrodynamic radius, R_H, of the PS_8P2VP_8 associates at pH 2 and at 25 °C (line is the linear fit). Inset: characteristic autocorrelation function (red line) along with the relaxation time distribution derived by CONTIN analysis of 0.1 mg/mL polymer concentration.

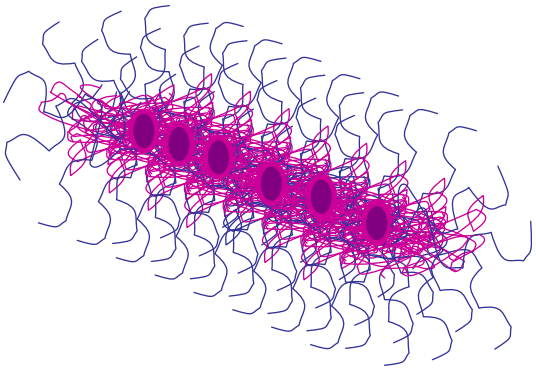

Scheme 2. Schematic representation of a colloidal soft nanoparticle made from self-organization of six PS_8P2VP_8 stars.

effects are expected to become significant. A continuous decrease of the diffusion coefficient with increasing concentration was observed (Fig. 5), as well as deviations of the first cumulants $\Gamma(q)$ from the q^2-dependence. The Γ versus q^2 plots (not shown) made it clear that the influence of center of mass diffusion had already significantly dropped, internal or segmental motions governing the behavior. Moreover the light scattering intensity levels off above c^*_{Rh}, which could mean that further association of the stars do not occur.

The more concentrated regimes were studied using rheological investigation techniques. The main objective of this part is to study how the entities revealed by light scattering experiments discussed in the previous section behave when crowding prevails.

3.2.1. Steady shear rheological properties

The apparent steady shear viscosity of the amphiphilic polyelectrolyte star in water has been plotted as a function of shear stress in Fig. 6, at pH 2. Below a polymer concentration of 2 wt%, the suspension behaves as a Newtonian fluid; at 3 wt%, the flow curve exhibits shear-thinning over the whole range of stresses explored, whereas above 3 wt%, a near discontinuity in the flow curve is observed at intermediate shear stresses, separating two smooth shear-thinning regions, a high-viscosity one at low stresses and a low-viscosity one at high stresses.

From a phenomenological point of view, the rheological behavior observed above 3 wt% is usually attributed to the existence of a so-called apparent yield stress, which marks the abrupt

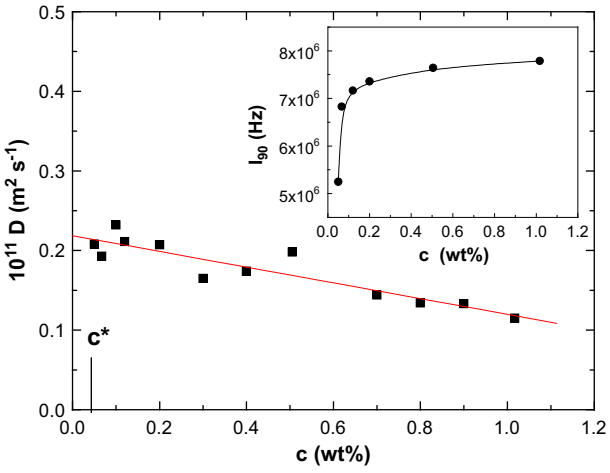

Fig. 5. Concentration dependence of the diffusion coefficient and static light scattering intensity (inset) determined at 90°, of the PS_8P2VP_8 aqueous solutions at pH 2 and at 25 °C in the semi dilute unentangled regime.

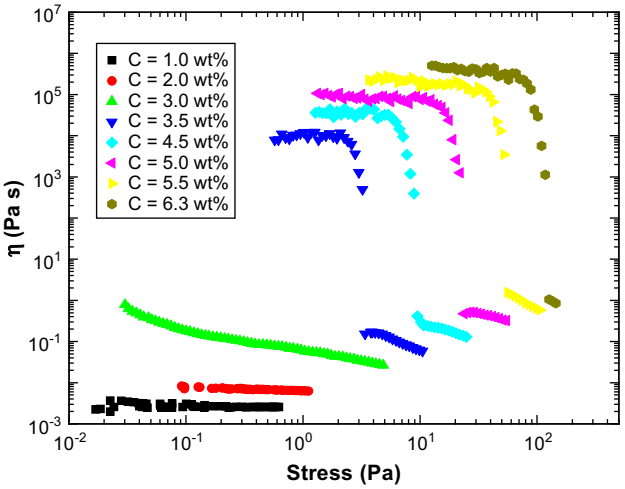

Fig. 6. Apparent viscosity as a function of shear stress for different polymer concentrations, at pH = 2 and at 25 °C.

transition between a very high viscosity flow behavior, and a low viscosity flow behavior [26]. Fig. 7, representing the apparent yield stress as a function of polymer concentration, shows that the apparent yield stress strongly increases with concentration above 3 wt%. Evidence of a sharp transition between 2 and 3 wt% is confirmed when plotting the apparent viscosity versus concentration. Fig. 8 shows the low-shear viscosity, η measured at 10^{-4} s^{-1} corresponding to the high-viscosity region of the flow curve, as a function of concentration c, at pH = 2. The absence of viscosity data at $c = 3$ wt% in Fig. 8 is due to the fact that it was impossible to measure the apparent viscosity of this sample at very low-shear rates $\sim 10^{-4}$ s^{-1}. The apparent viscosity versus concentration curve clearly exhibits a transition at a polymer concentration of about 2 wt%, characterized by a very sharp increase of the low-shear apparent viscosity (6 orders of magnitude), which looks like a near discontinuity in the vicinity of 3 wt%. Below $c = 2$ wt%, the apparent viscosity increases weakly with polymer concentration. At polymer concentrations higher than 3 wt%, the Newtonian viscosity increases strongly with concentration, following the empirical power law $\eta \propto c^{6.7}$.

3.2.2. Linear viscoelastic properties

For all samples at concentrations above 3 wt%, the strain dependency of both viscoelastic moduli (not shown in the paper)

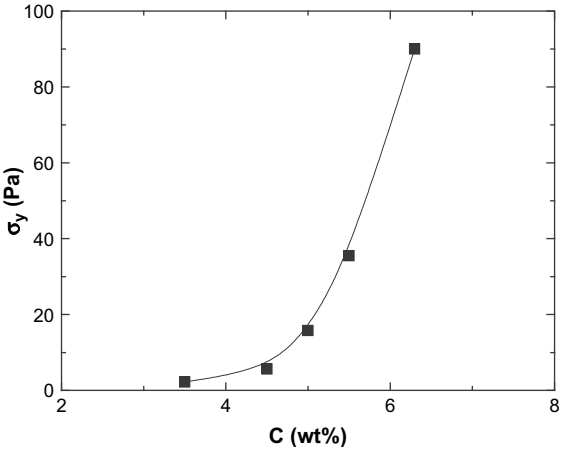

Fig. 7. Concentration dependence of the apparent yield stress of the hydrogel formed at pH 2 and 25 °C.

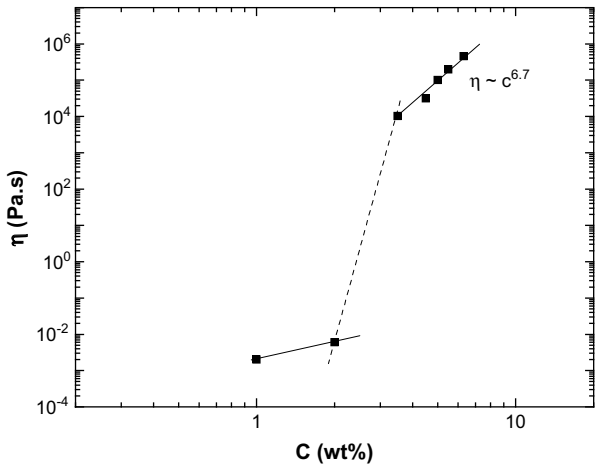

Fig. 8. Low-shear apparent viscosity as a function of polymer concentration, at pH 2 and at 25 °C.

does not exhibit any strain hardening behavior and the linear viscoelastic regime was shown to be limited to rather small strains, that is ~1%. Both viscoelastic moduli G' and G'', determined in the linear viscoelastic regime, were shown to be nearly independent of frequency (inset of Fig. 9). Moreover, G' was shown to be superior to G'' by about 1 decade for all samples tested. These results prove that the system studied behaves like an elastic soft solid at high concentrations. Moreover, Fig. 9 shows that the plateau storage modulus G'_0 is a power law function of the polymer concentration, with a power law exponent of about 5.4. The rheological investigation performed on concentrated suspensions shows the existence of a threshold polymer concentration of about 2 wt%, which marks the transition from a fluid like to a solid like behavior, as evidenced by the drastic increase of the apparent low-shear viscosity, coupled with the presence of an apparent yield stress and a frequency-independent storage modulus.

Colloidal systems with an attractive interparticle energy, exhibit such a fluid to solid transition at some threshold concentration due to colloidal gelation [27,28]. Colloidal particles having only a repulsive interaction on contact, also exhibit a fluid to solid transition: they undergo a glass transition to a disordered solid [29]. Similarities between colloidal gelation and glass transition are numerous, since they are both driven by crowding: crowding of

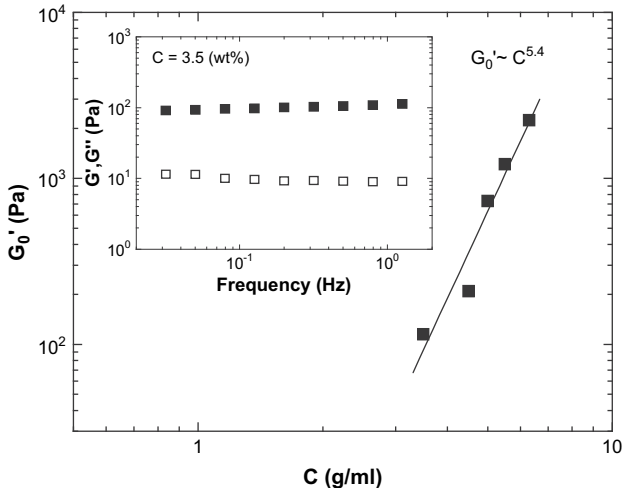

Fig. 9. Plateau storage modulus as a function of polymer concentration at pH 2. Inset: storage and loss modulus of a 3.5 wt% polymer solution as a function of frequency.

individual particles or crowding of particle aggregates [30], which induces structural arrest in the system. Unifying schemes have been proposed recently in order to describe such frozen systems, as reviewed by Trappe and Sandkühler [31]. Particular interest was shown in the concept of jamming [32], which proved to be a good conceptual framework for describing soft glassy materials [33].

A significant finding of the present system is that the concentration where the fluid to solid like transition occurs was observed about 40 times higher than the hydrodynamic overlap concentration. This behavior should be ascribed to the charged character of the star-like colloidal soft nanoparticles. According to recent theoretical considerations for multiarm star polyelectrolyte solutions, several concentration regimes have been identified [14]. Above the overlap concentration, an extended concentration regime, named *overlap* regime, was predicted where the stars do not interdigitate. In this regime, the star radius decreases with concentration (compaction effect) because the arm stretching has to disappear in order to make the interdigitation favorable. The compaction regime continues until the size of the arms decreases to the size of a linear chain in a semi dilute regime. In this case the electrostatic interactions have been screened and the stars behave like neutral stars.

As reported previously [34], neutral multiarm star polymers have been clearly proved to behave as more or less soft colloidal nanoparticles in organic solvents. More precisely in a dense star suspension, an increase of temperature leads to star overlap enhancement, interdigitation and jamming which causes dynamic arrest of the suspension. Hence it is suggested that the fluid to solid transition observed herein is another example of jamming transition, even though very slow dynamics and aging effects, which are often seen as rheological signatures of jammed systems [35] have not been studied in the present work.

4. Conclusions

We have explored the ability of amphiphilic heteroarm polyelectrolyte stars, constituted of pure polystyrene and poly(2-vinyl pyridine) arms, to form colloidal gel in acidic salt-free aqueous media. The low concentration regime was investigated by static and dynamic light scattering and the concentrated properties were studied by rheometry. The results showed that intermolecular hydrophobic association prevails in the dilute regime, where colloidal soft nanoparticles constituted of about 6 stars are formed. Far above the overlap concentration determined at 0.046 wt%, (i.e. at about $40c^*$), a fluid to soft solid transition was observed, leading to a colloidal gel due to crowding effects (jamming transition). In the extended concentration regime between the hydrodynamic overlap concentration and the jamming transition, a continuous compaction of the star-like soft nanoparticles prior to interdigitation seems to occur, in qualitative agreement with the scaling theory for star polyelectrolytes [14].

Acknowledgement

The present work was performed within the framework of the 2006/2007 French–Greek "Platon" PHC Project no. 11299 RH. T. Aubry and C. Tsitsilianis acknowledge financial support of the French Ministry of Foreign Affairs and the Greek Ministry of Development.

References

[1] Bhatia SR, Mourchid A, Joanicot M. Curr Opin Colloid Interface Sci 2001; 6:471.
[2] Alexandridis P, Lindman B. Amphiphilic block copolymers: self assembly and applications. New York: Elsevier; 2000.
[3] Vlassopoulos D, Fytas G, Pispas S, Hadjichristidis N. Physica B 2001;296:184.

[4] Daoud M, Cotton JP. J Phys, France 1982;43:531.
[5] Milner ST, McLeish TCB. Macromolecules 1997;30:2159.
[6] Marques CM, Izzo D, Charitat T, Mendes E. Eur Phys J B 1998;3:353.
[7] Miros A, Vlassopoulos D, Likhtman AE, Roovers J. J Rheol 2003;47:163.
[8] Birshtein TM, Zhulina EB, Borisov OV. Polymer 1986;27:1078.
[9] Vlassopoulos D, Fytas G, Pakula T, Roovers J. J Phys Condens Matter 2001;13:855.
[10] Kapnistos M, Semenov AN, Vlassopoulos D, Roovers J. J Chem Phys 1999; 111:1753.
[11] Pincus P. Macromolecules 1991;24:2912.
[12] Borisov OV, Zhulina EB. Eur Phys J B 1998;4:205.
[13] Korobko AV, Jesse W, Lapp A, Egelhaff SU, van derr Maarel JRC. J Chem Phys 2005;122:24902.
[14] Shusharina NP, Rubinstein M. Macromolecules 2008;41:203.
[15] (a) Tsitsilianis C, Chaumont Ph, Rempp P. Makromol Chem 1990;191:2319;
(b) Tsitsilianis C. Macromolecules 1993;26:2977;
(c) Grayer V, Dormidontova EE, Hadziioannou G, Tsitsilianis C. Macromolecules 2000;33:6330;
(d) Gorodyska A, Kiriy A, Minko S, Tsitsilianis C, Stamm M. Nano Lett 2003; 3:365.
[16] Voulgaris D, Tsitsilianis C. Macromol Chem Phys 2001;202:3284–92.
[17] Štěpánek M, Matějíček P, Humpolíčková J, Havránková J, Prodhájecká K, Špírková M, et al. Polymer 2005;46:10493.
[18] Tsitsilianis C, Voulgaris D. Macromol Chem Phys 1997;198:997.
[19] Tsitsilianis C, Voulgaris D, Stěpánek M, Prodhájecká K, Procházka K, Tuzar Z, et al. Langmuir 2000;16:6868–76.
[20] Kiriy A, Gorodyska A, Minko S, Stamm M, Tsitsilianis C. Macromolecules 2003; 36:8704.
[21] (a) Burchard W. Biomacromolecules 2001;2:342;
(b) Zimm BH. J Chem Phys 1948;16:1093.
[22] Antoniety M, Heiz S, Schmidt M, Rosenauer C. Macromolecules 1994;27:3276.
[23] (a) Jusufi A, Likos CN, Löwen H. J Chem Phys 2002;116:11011;
(b) Jusufi A, Likos CN, Löwen H. Phys Rev Lett 2002;88:018301;
(c) Jusufi A, Likos CN, Ballauff. Colloid Polym Sci 2004;282:910.
[24] (a) Wittemann A, Drechsler M, Talmon Y, Ballauff M. J Am Chem Soc 2005; 127:9688;
(b) Ballauff M, Borisov O. Curr Opin Colloid Interface Sci 2006;11:316.
[25] Likos CN, Blaak R, Wynveen A. J Phys Condens Matter 2008;20:494221.
[26] Barnes HA, Walters K. Rheologica Acta 1985;24:323.
[27] Chen M, Russel WB. J Colloid Interface Sci 1997;141:564.
[28] Yanez JA, Laarz E, Bergstrom L. J Colloid Interface Sci 1999;209:162.
[29] van Megen W, Underwood SM. Phys Rev E 1994;49:4206.
[30] Segré PN, Prasad V, Schofield AB, Weitz DA. Phys Rev Lett 2001;86:6042.
[31] Trappe V, Sandkühler P. Curr Opin Colloid Interface Sci 2004;8:494.
[32] Liu AJ, Nagel SR. Nature 1998;396:21.
[33] Trappe V, Prasad V, Cipelletti L, Ségre PN, Weitz DA. Nature 2001;471:772.
[34] Vlassopoulos D. J Polym Sci Part B Polym Phys 2004;42:2931.
[35] Cipeleletti L, Ramos L. Curr Opin Colloid Interface Sci 2002;7:228.